NASA TECHNICAL MEMORANDUM

NASA TM X-71677

NASA TM X-71677

(NASA-TM-X-71677) DETERMINATION OF ELECTRON TEMPERATURE IN A PENNING DISCHARGE BY THE HELIUM LINE RATIO METHOD (NASA) 21 p HC $3.25 CSCL 20I

N75-24478

Unclas G3/75 21833

DETERMINATION OF ELECTRON TEMPERATURE IN A PENNING DISCHARGE BY THE HELIUM LINE RATIO METHOD

by Richard W. Richardson
Lewis Research Center
Cleveland, Ohio 44135

TECHNICAL PAPER to be presented at
Second International Conference on Plasma Science
sponsored by Institute of Electrical and Electronics Engineers
Ann Arbor, Michigan, May 14-16, 1975

E-8271

DETERMINATION OF ELECTRON TEMPERATURE IN A PENNING DISCHARGE BY THE HELIUM LINE RATIO METHOD

by Richard W. Richardson*

NASA Lewis Research Center

Cleveland, Ohio 44135

In this experiment, the helium line ratio technique is used to determine electron temperatures in a toroidal steady-state Penning discharge operating in helium. Due to the low background pressure, less than 10^{-4} Torr, and the low electron density (believed to be less than 10^{10} cm^{-3}), the corona model is expected to provide a good description of the excitation processes in this discharge. In addition, by varying the Penning discharge anode voltage and background pressure, it is possible to vary the electron temperature as measured by the line ratio technique over a wide range (10 to 100+ eV). These discharge characteristics have allowed a detailed comparison of electron temperatures measured from different possible line ratios over a wide range of temperatures and under reproducible steady-state conditions. Good agreement is found between temperatures determined from different neutral line ratios, but use of the helium ion line results in a temperature systematically 10 eV high compared to that from the neutral lines. This discrepancy is believed to be due to an enhanced tail on the electron energy distribution or an unresolved systematic error in the application of the technique involving the He^+ line.

---

*NASA-NRC Post Doctoral Research Associate.

INTRODUCTION

The helium spectral line intensity ratio technique can be used to determine the electron temperature in a corona model plasma (refs. 1 to 3). This technique utilizes the difference in electron energy dependences of the ground state electron impact excitation cross sections of the singlet and triplet series of neutral helium and also the excited states of helium ions. In this experiment the helium line ratio technique is used to determine electron temperatures in a toroidal steady-state Penning discharge (ref. 4) operating in helium. Due to the low background pressure, less than 10^{-4} Torr, and the low electron density, believed to be less than 10^{10} cm^{-3}, the corona model (ref. 5) is expected to provide a good description of the excitation processes in this discharge. The line ratio technique should therefore be free of the limitations described by Sovie (ref. 6). In addition, by varying the Penning discharge anode voltage and background pressure, it is possible to vary the electron temperature as measured by the line ratio technique from 10 to 100+ eV. Thus it has been possible to make a comparison of the electron temperature as measured from different possible line ratios over a wide range of temperatures under reproducible steady-state conditions.

EXPERIMENT

Discharge

The toroidal Penning discharge is produced in the NASA Lewis Bumpy Torus magnet facility (refs. 7 and 8). The bumpy torus has a major diameter of 1.52 meters and was operated with a maximum magnetic flux at the mirror throats of 2.4 Tesla. The discharge is approximately 82 liters in volume and is produced by an 18 cm diameter anode ring maintained at high voltage in each of the twelve magnetic mirror midplanes (see fig. 1). The discharge boundary is well defined by the intersection of lines of magnetic flux with the inside edge of the anode rings and is well away from the vacuum tank walls. The cold cathodes for the discharge are the grounded magnet coil bores which are outside the observed plasma boundary. It is believed that the current path to ground is completed by ions lost across the plasma boundary to the cathodes rather than by secondary electrons crossing the strong magnetic flux region into the discharge. This is advantageous from the standpoint of the spectroscopic measurement since a beam of high energy secondary electrons is not expected to exist in the discharge. The discharge was operated for these measurements over a range of anode voltages and background pressures of 2.5 to 28 kV and 0.5×10^{-5} to 10^{-4} Torr, respectively.

This discharge in this operating regime is known to produce Maxwellian ion energy distributions with kinetic temperatures of several hundred eV to several keV resulting apparently from charge drift in the crossed electric and magnetic fields and randomization of the drift energy by strong electrostatic potential fluctuations (refs. 9-11). The electrons are expected to be at a much lower temperature due to the similar drift velocity to that of the ions and the unimportance of electron-ion thermalizing collisions at these low densities. It is anticipated that the electron energy distribution is Maxwellianized by the same process as the ions.

Measurement of Spectral Intensities

A schematic of the spectroscopic apparatus is shown in figure 1. A thin horizontal chord through the plasma was viewed with imaging optics. The observation was made perpendicular to the magnetic flux at a magnetic mirror midplane between a special double anode ring as indicated in figure 1. The two anodes were placed 3 cm apart. Chords at different vertical positions could be observed by translation of the imaging lens perpendicular to the optical axis. Line intensities in the visible helium spectrum were measured with a 1.5 meter Fastie-Ebert spectrometer with a photomultiplier tube output. Output currents were time integrated with a time constant of several seconds. The spectrum was scanned in the vicinity of each spectral line to allow determination of the baseline and line peak. The line intensity was taken to be the difference between the line peak and baseline. A standard lamp was used to determine the spectral response of the entire system. Entrance and exit slits of 100 microns were used for all measurements. No broadening of the spectral lines other than instrument broadening (1 Å) was observed.

Determination of Electron Temperature

Assuming a weakly ionized, corona model plasma and a Maxwellian electron energy distribution, the measured relative intensity,

$I_{jk}(y)$, of a spectral line due to a transition $j \rightarrow k$ at a chord position y observing across an axisymmetric cylindrical source is given by the expression

$$kI_{jk} = 2\int_0^{\sqrt{R^2-y^2}} n(r)n_o < \sigma_{jk}(v)v > dl \qquad (1)$$

where R is the discharge radius and dl is a length of chord. Here I_{jk} is defined to be the relative number of radiative transitions per second consistent with references 1, 2, and 6. Also $< \sigma_{jk}(v)v > = S_{jk}(T_e)$ is the apparent optical line excitation rate coefficient for excitation from the neutral ground state, $\sigma_{jk}(v)$ being the apparent cross section as a function of electron velocity, v, and the angle brackets indicate an average over a Maxwellian distribution of electrons of kinetic temperature T_e. The quantity $n(r)$ is the electron density as a function of radius, r, n_o is the background neutral density, and k is the absolute calibration factor of the optical system (the relative calibration is included in I_{jk}). If T_e is constant across the chord, the ratio of two line intensities with different electron energy dependences gives

$$\frac{I_{jk}(y)}{I_{lm}(y)} = \frac{S_{jk}(T_e)}{S_{lm}(T_e)} \qquad (2)$$

which can be used to determine T_e (refs. 1 to 3) if experimental $\sigma_{jk}(v)$ are known. Previously, in this discharge, Abel inversions of the $I_{jk}(y)$ have been used to eliminate the integral in equation (1) and determine $T_e(r)$ (ref. 12). The electron temperature was observed to increase in the region near the anode. The T_e determined from equation (2) was found to be consistent with the temperature in the main body of the plasma.

The criteria set forth by Sovie (ref. 6) for neglecting the effect of electron collisional depopulation of the observed states and population by electron excitation from the metastable states and radiative recombination are found to be well satisfied here due to the low background pressure and electron density. These will be discussed later.

In this discharge the values of T_e range from near the excitation energy for neutral excitation to greater than 100 eV. The excitation of neutrals is thus from the bulk of the electron distribution and the resulting excitation rates are not sensitive to anomalies in the tail of the distribution. This is not necessarily true for the He^+ (468.6 nm) line which has a threshold at 70 eV and peaks at 200 eV. At lower electron temperatures (such as in a glow discharge) the assumption of a Maxwellian tail may lead to erroneous results.

Cross Sections

With regards to the choice of transitions to observe, Sovie (ref. 1) has suggested use of transitions from the n^1S and n^3S neutral helium levels since they are known from cross section measurements to be least sensitive to background pressure. At low electron densities $(n/n_o \ll 1)$ excitation of He^+ states is predominantly from the neutral ground state and equation (2) is valid for combinations of neutral and ionic states. The most recent measurement of cross sections and calculation of rate coefficients for use with this technique are given by Latimer (ref. 2) for the 504.8 nm ($2^1p - 4^1s$), 443.8 nm ($2^1p - 5^1s$), 471.3 nm ($2^1p - 4^3s$), and 412.1 nm ($2^1p - 5^1s$) neutral lines and for the He^+ (3 - 4) 468.6 nm line.

The triplet cross sections used in reference 2 (the same as ref. 13) have come under question due to the belief that the triplet states should be excited by electron exchange and the high energy portion (above ~50 eV) fall off as E^{-3} (ref. 14), E being electron energy, much faster than observed in references 2 and 13. The more recent results of reference 14 indicate an n^3S cross section which does fall off as E^{-3}. Therefore, the E^{-3} dependence has been normalized to the cross section used by Latimer (ref. 13) at 50 eV and the rate coefficients and ratios recalculated. The recalculated ratios for the 504.8 nm, 471.3 nm, and 468.6 nm lines are shown in figure 2 and compared with the previous calculation of reference 2. The correction becomes significant at $T_e > 40$ eV.

Since the cross section energy dependences are found to be essentially the same within the n^1S and n^3S levels, respectively, the ratios in figure 2 also apply to other lines (such as the 443.8 nm and 412.1 nm lines) when multiplied by the appropriate ratio of maximum cross sections of the various lines.

RESULTS AND DISCUSSION

By varying the Penning discharge anode voltage and background pressure, the electron temperature as measured by the line ratio technique has been varied over a wide range (10 to 100+ eV). Electron temperatures as determined from various possible line ratios using the revised triplet cross sections over the range of conditions have been compared in the following figures.

Figure 3 compares T_e measured by the ratio of the 504.8 nm and 471.3 nm neutral line intensities to that measured from the 443.8 nm and 412.1 nm line intensities for the same set of operating conditions. This comparison is shown in figure 3 for some 170 sets of operating conditions each represented by a symbol. For perfect agreement all points would lie along the 45° line. Also shown are several points determined by Latimer et al. (ref. 2) corrected for the revised cross section. The same set of data has been analyzed statistically by forming the ratio of the two temperatures, determining the median value of the ratio over all operating conditions, and plotting the ratio normalized to the median on the cumulative probability plot of figure 4. This gives a median of 1.08 and a standard deviation of ±9 percent, the points lying approximately along a Gaussian distribution as represented by the straight line in figure 4. The two temperatures as determined from the neutral lines thus agree within the random error over the range of temperatures. The observed random error of ±9 percent is indicative of the measurement accuracy. The agreement in figure 3 is expected if the spectral calibration and measured maximum cross sections are correct (at least relative to one another), and the cross section energy dependences are similar within the n^1S and n^3S series, respectively, as indicated by the cross section measurements (differing only in maximum value of the cross section). It cannot be deduced from figure 3 that the choice of a Maxwellian distribution or the measured cross sections, and hence the electron temperatures, are necessarily correct. An agreement similar to figure 3 is observed if the ratios of Latimer (ref. 2) are used, but the individual temperatures are significantly higher.

Since, as mentioned, the cross section energy dependences are the same within the n^1S and n^3S series, respectively, the ratio of the intensities of various $2^1P - n^1S$ transitions should be equal to the ratio of their maximum cross sections independent of T_e, unless another depopulation process is occurring (ref. 6). To investigate this, the quantity $I(2^1P - n^1S)\sigma(2^1P - 4^1S)/I(2^1P - 4^1S)\sigma(2^1P - n^1S)$ for $n = 5$, 6, and 8 is plotted versus the estimated relative electron density, $\overline{n} = I_{jk}/n_o S_{jk}(T_e)$ in figure 5. The ratio for $n = 5$, the highest state used for determination of T_e, is observed to fall off only slightly at highest $\overline{n}$. The 416.9 nm ($2^1P - 6^1S$) and 393.6 nm ($2^1P - 8^1S$) transitions were observed for only a small number of operating conditions. The ratios for $n = 6$ and especially $n = 8$ are observed to fall distinctly below one at higher $\overline{n}$ indicating the onset of collisional depopulation. The higher states are expected to be affected more strongly due to the longer lifetimes of these states (the lifetime of the 8^1S state being 13.5 times as long as the 5^1S state) making an electron collision more probable.

The measured cross sections and energy distribution function can be considered by comparing the three temperatures which can be determined from various ratios of one of the singlet lines, one of the triplet lines, and the He^+ line. Due to the similarity of the cross section energy dependences within a series, the additional singlet and triplet lines observed are redundant with regards to this type of comparison and do not supply additional information beyond that already discussed.

In figure 6(a) the temperatures as measured from the ratio of the 468.6 nm (3 - 4) He^+ line intensity to the 471.3 triplet neutral helium intensity is plotted versus that measured from the 504.8 nm to 471.3 nm neutral helium ratio. The temperature measured using the He^+ line is systematically 10 eV high over the entire range of temperatures. Figure 6(b) shows the temperature determined from the 504.8 nm singlet intensity ratioed with the He^+ line as compared to that determined from the 504.8 nm and 471.3 nm neutral line ratio. Again the He^+ temperature is systematically high. Figure 6(c) shows that temperatures determined from the 504.8 nm and 471.3 nm lines, respectively, ratioed with the He^+ line are in considerably better agreement. Also shown in figures 6(a) and (c) are the temperatures as measured by Latimer (ref. 2) over a similar range adjusted to the revised cross sections. A similar systematic error is evident. The effect of using the ratio calculations of Latimer are shown in figure 7, equivalent to figure 6(a). The systematic discrepancy is similar at low T_e but reverses at high T_e, the overall situation not being improved.

The same discrepancy is observed when the T_e determined from the He^+ line ratioed with a singlet or triplet line is compared to T_e

determined from the singlet to triplet line ratio. The major discrepancy at low temperature disappears when comparing temperatures each measured with the He^+ line. Since in each case, figures 6(a) and (c), the effect of the line intensity common to each axis will tend to be compensating, it is believed that the singlet and triplet cross sections are not the source of the discrepancy. Reference to figure 2 shows that for the low range of temperatures, the intensity ratio involving the He^+ line essentially asymptotes at about $T_e = 20$ eV. This means that a small error in the measured cross section f the He^+ line (equivalent to an error in measuring the He^+ line intensity, say, due to underlying impurity) will have negligible effect on the measured T_e at low temperature and a larger effect at high temperatures. This is opposite to the effect required to explain the trend of data in figures 6(a) and (c). At the lowest T_e as measured by the neutral lines, 13 eV, the He^+ line, according to figure 2, should be essentially unobservable compared to the neutral lines. Even a rather large error in the measured cross section of the 468.6 nm line would not resolve this discrepancy.

The discrepancy could result from the ion line being predominantly excited from the ion ground state. Excitation from the neutral ground state has been assumed. The condition that the excitation of the He^+ live be predominantly from the neutral ground state is that $n >> n_o S_{4,3}/S^+_{4,3}$ where g and + refer to excitation from the neutral ground state and ion ground state, respectively. Using $S^+_{4,3}$

as calculated in reference 1 gives, at a minimum, $n \gg 5 \times 10^{11}$ cm^{-3}. The density in this device is believed to be one to two orders of magnitude lower for these operating conditions. In addition, Doppler broadening of the line if excited from the ion ground state should be significant as compared to instrument broadening at keV ion temperatures and is not observed. The decay time of the He^+ state is sufficiently short ($\sim 10^{-9}$ sec) that a newly created ion accelerated by estimated plasma electric fields before decay is not expected to lead to significant Doppler broadening.

Considering this experiment alone, an enhanced tail on the electron energy distribution seems the most probable source of the discrepancy. An enhancement in the tail near the He^+ line cross section peak at 200 eV of the order of 1 percent of the total electron density would be sufficient to cause the discrepancy. (The possibility of excitation of neutrals by the high temperature ions leading to such a discrepancy cannot be completely ruled out. This process cannot be estimated quantitatively due to the lack of known cross sections for excitations of helium neutrals by helium ions.) It has been noted that a similar discrepancy is observed in the results of Latimer (ref. 2) for a quite different experimental situation. For this reason it seems that an unresolved systematic error in the application of the technique involving the He^+ line cannot be disregarded. An understanding of the source of the disagreement would be valuable since the comparative intensity of the ion line is useful for making definite statements about the distribution function and even measuring the percentage ionization as suggested by Sovie (ref. 1). The latter, at least in this experiment, apparently leads to a gross overestimate of the percentage ionization.

REFERENCES

1. R. J. Sovie, "Spectroscopic Determination of Electron Temperature and Percentage Ionization in a Helium Plasma," Phys. Fluids, vol. 7, pp. 613-614, 1964.

2. I. D. Latimer, J. I. Mills, and R. A. Day, "Refinements in the Helium Line Ratio Technique for Electron Temperature Measurement and Its Application to the Precursor," J. Quant. Spectr. Rad. Trans., vol. 10, pp. 629-635, 1970.

3. R. H. Huddlestone and S. L. Leonard, eds., Plasma Diagnostic Techniques. Academic Press, 1965, p. 254.

4. J. R. Roth, R. W. Richardson, and G. A. Gerdin, "Initial Results from the NASA Lewis Bumpy Torus Experiment," presented at American Physical Society, Annual Meeting, Philadelphia, Pa., Oct. 30-Nov. 4, 1973.

5. R. H. Huddlestone and S. L. Leonard, eds., Plasma Diagnostic Techniques. Academic Press, 1965, pp. 208-214.

6. R. J. Sovie, "The Effects of Cascading and Metastable Atoms on the Determination of Electron Temperature from Relative Line Intensities in a Tenuous Helium Plasma," J. Quant. Spectr. Rad. Trans., vol. 8, pp. 833-838, 1968.

7. J. R. Roth, A. D. Holmes, T. A. Keller, and W. M. Krawczonek, "Characteristics and Performance of a 12-Coil Superconducting "Bumpy Torus" Magnet Facility for Plasma Research," National Aeronautics and Space Administration, Washington, D.C., Tech. Note D-7353, Aug. 1973.

8. J. R. Roth, A. D. Holmes, T. A. Keller, and W. M. Krawczonek, "A 12-Coil Superconducting "Bumpy Torus" Magnet Facility for Plasma Research," in IEEE Proc. 1972 Applied Superconductivity Conf., pp. 361-366, May 1972.

9. J. R. Roth, "Hot Ion Production in a Modified Penning Discharge," IEEE Trans. Plasma Sci., vol. 1, pp. 34-45, 1973.

10. J. R. Roth, "Energy Distribution Functions of Kilovolt Ions in a Modified Penning Dishcarge," Plasma Phys., vol. 15, pp. 995-1005, 1973.

11. J. R. Roth, "Origin of Hot Ions Observed in a Modified Penning Discharge," Phys. Fluids, vol. 16, pp. 231-236, 1973.

12. R. W. Richardson, "Spectroscopic Results in Helium from the NASA Lewis Bumpy Torus," presented at Institute of Electrical and Electronics Engineers International Conference on Plasma Science, 1st, Knoxville, Tenn., May 15-17, 1974.

13. I. D. Latimer, private communication.

14. R. B. Kay and J. G. Showalter, "Exchange Excitation in Helium: Excitation Functions for the 4^3S, 3^3P, and 3^3D Levels," Phys. Rev. A., vol. 3, pp. 1998-2006, June 1971.

E-8271

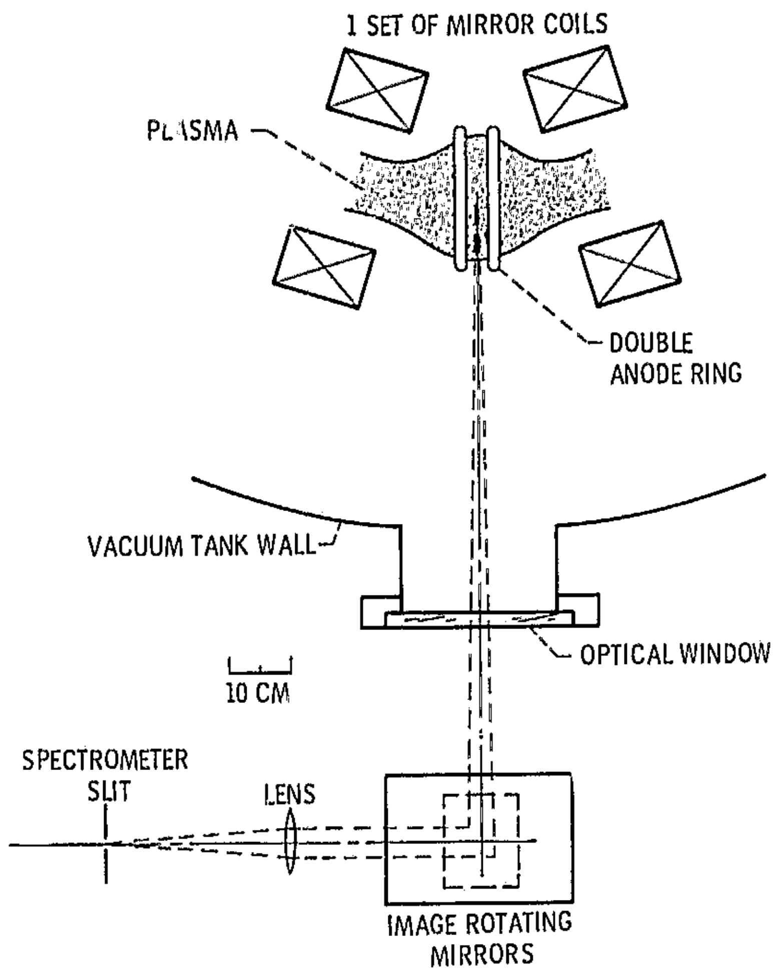

Figure 1. - Schematic drawing of the experimental apparatus.

E-8271

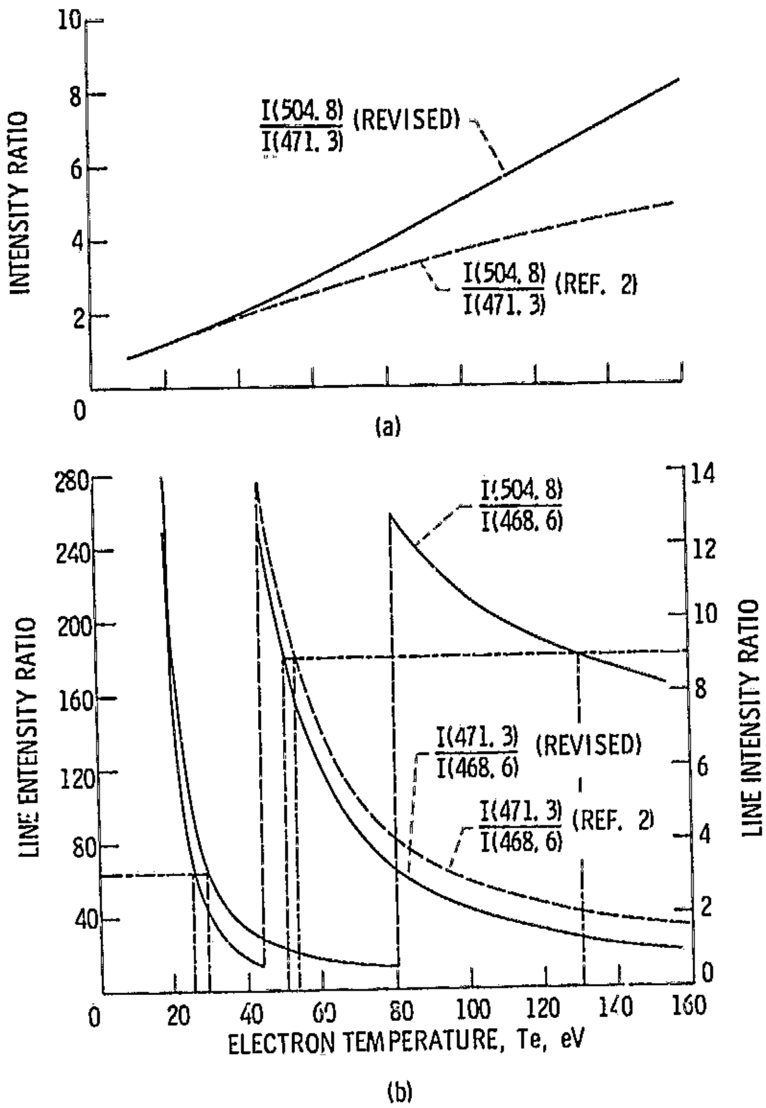

Figure 2. - Line intensity ratio - electron temperature.

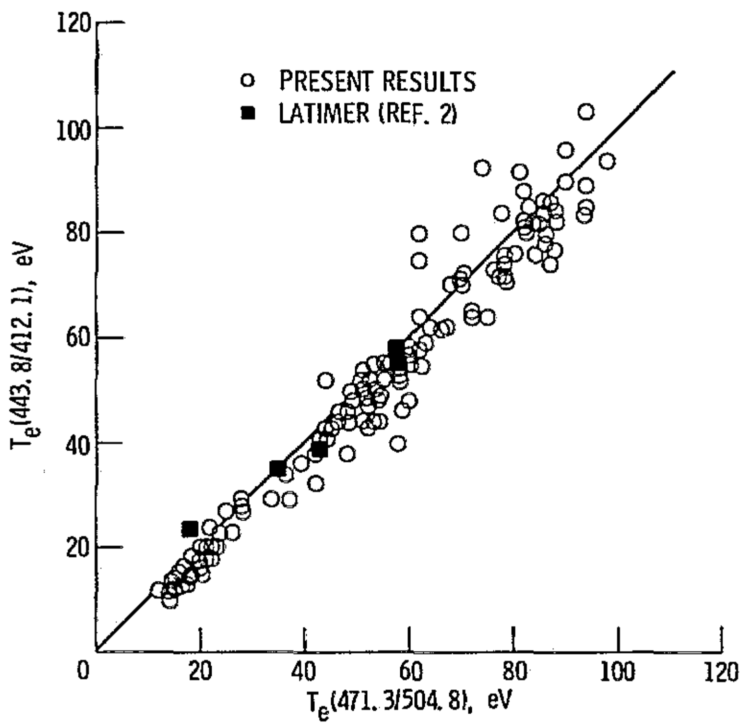

Figure 3. - Electron temperature comparison.

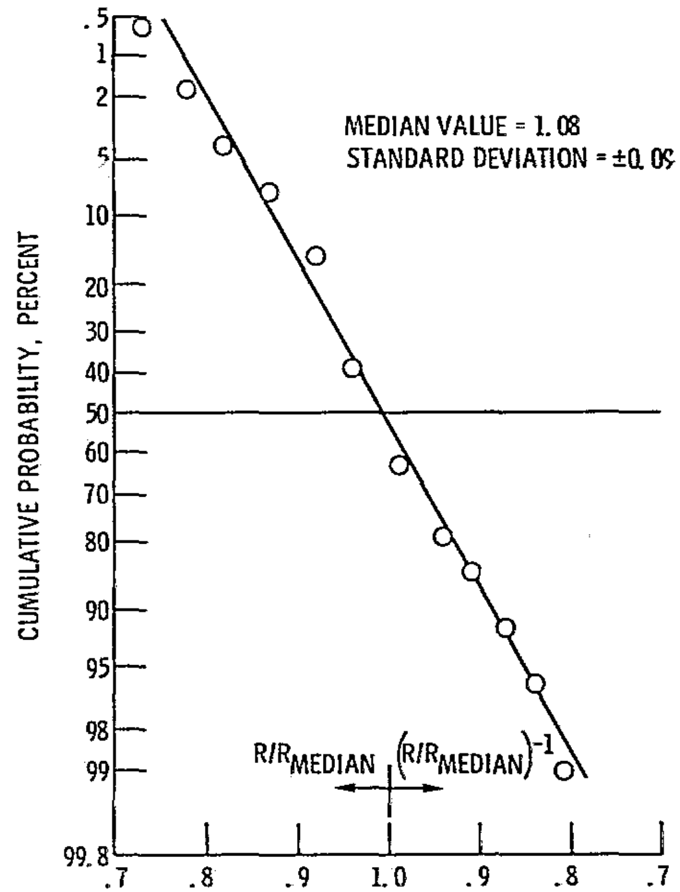

Figure 4. - Cumulative probability plot.

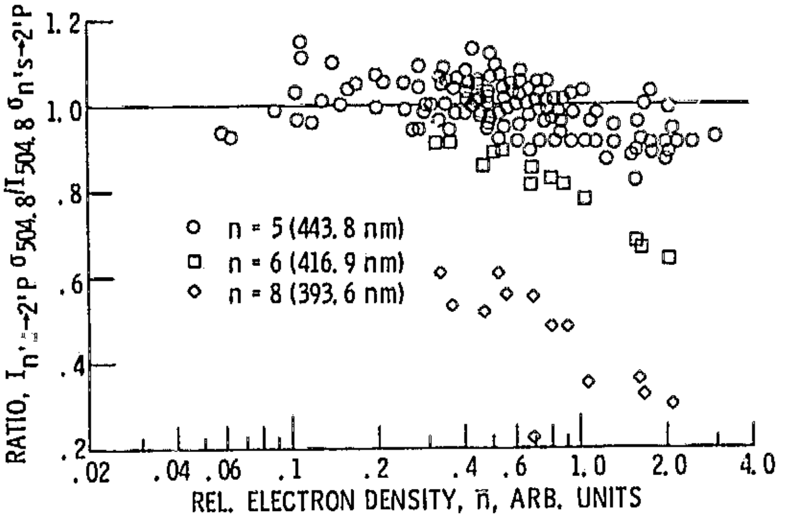

Figure 5. - Singlet intensity ratios.

E-8271

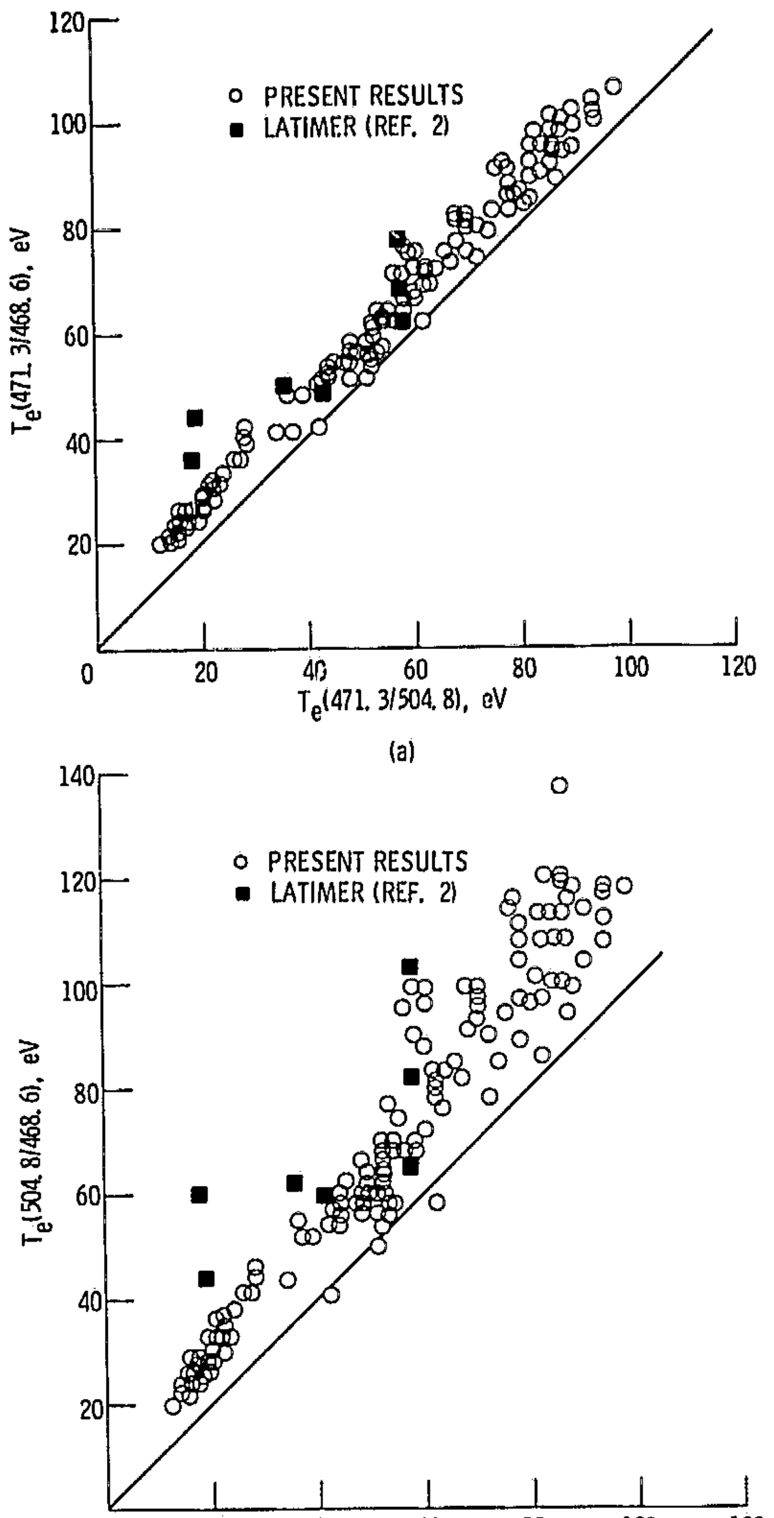

Figure 6. - Electron temperature comparison.

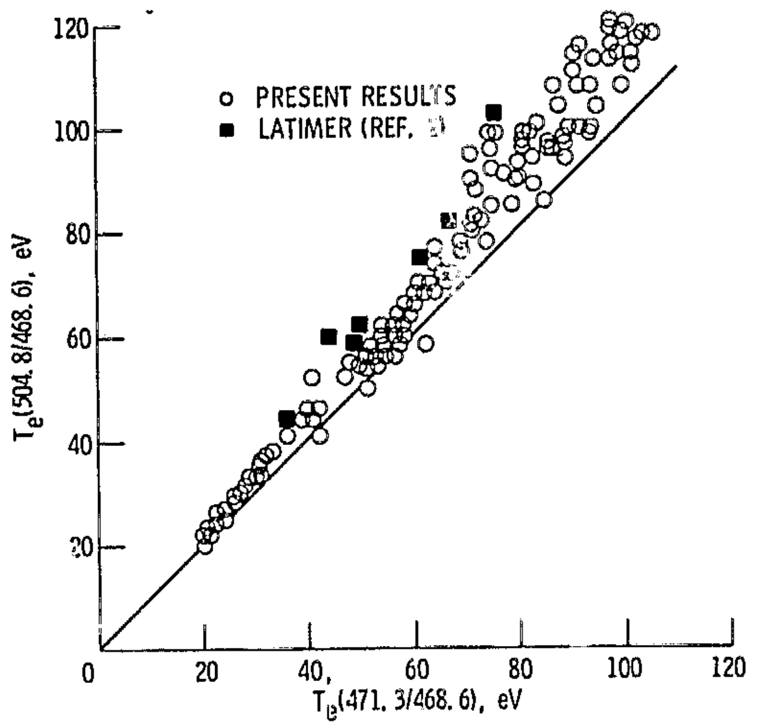

(c)

Figure 6. - Concluded.

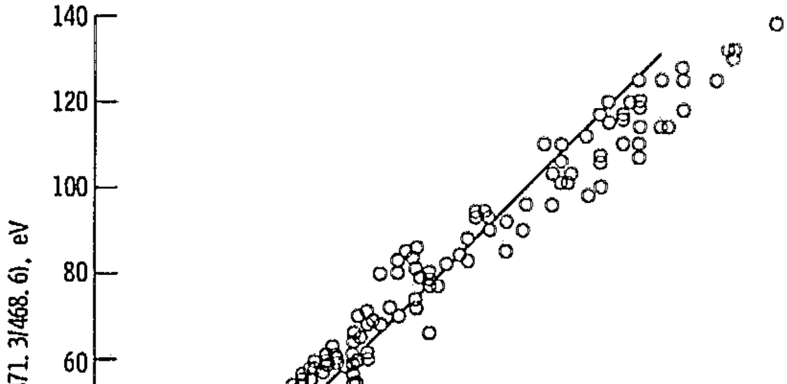

Figure 7. - Electron temperature comparison.

E-8271